Heat Shock Protein 70 Surface-Positive Tumor Exosomes Stimulate Migratory and Cytolytic Activity of Natural Killer Cells

Robert Gastpar[1], **Mathias Gehrmann**[1], **Maria A. Bausero**[3], **Alexzander Asea**[3], **Catharina Gross**[1], **Josef A. Schroeder**[2], and **Gabriele Multhoff**[1]

1*Department of Hematology and Oncology, University Hospital Regensburg, Regensburg, Germany*

2*Institute of Pathology, University Hospital Regensburg, Regensburg, Germany*

3*Center for Molecular Stress Response, Boston University Medical Center and Boston University School of Medicine, Boston, Massachusetts*

Abstract

Detergent-soluble membrane vesicles are actively released by human pancreas (Colo−/Colo+) and colon (CX−/CX+) carcinoma sublines, differing in their capacity to present heat shock protein 70 (Hsp70)/Bag-4 on their plasma membranes. Floating properties, acetylcholine esterase activity, and protein composition characterized them as exosomes. An enrichment of Rab-4 documented their intracellular transport route from early endosomes to the plasma membrane. After solubilization, comparable amounts of cytosolic proteins, including tubulin, Hsp70, Hsc70, and Bag-4, but not ER-residing Grp94 and calnexin, were detectable in tumor-derived exosomes. However, with respect to the exosomal surface, only Colo+/CX+ but not Colo−/CX exosomes were Hsp70 membrane derived positive. Therefore, concomitant with an up-regulated cell surface density of activation markers, migration and Hsp70 reactivity of natural killer (NK) cells was stimulated selectively by Hsp70/Bag-4 surface-positive exosomes, but not by their negative counterparts and tumor cell lysates. Moreover, the exosome-mediated lytic activity of NK cells was blockable by Hsp70-specific antibody. As already shown for TKD stimulation, NK cells preincubated with Hsp70 surface-positive exosomes initiated apoptosis in tumors through granzyme B release. In summary, our data provide an explanation how Hsp70 reactivity in NK cells is induced by tumor-derived exosomes.

Introduction

Heat shock proteins (HSP) inhabit nearly all cellular compartments, where they support folding of nascent polypeptides, prevent protein aggregation, and assist transport of other proteins across membranes (1). Our group determined a tumor-specific plasma membrane localization of Hsp70, the major stress-inducible member of the HSP70 family (2). This finding was in line with data showing an abundance of molecular chaperones on tumor cell lines measured by global profiling of membrane-bound proteins (3). Although the exact mechanisms underlying transport of Hsp70 from the cytosol to the plasma membrane remains to be elucidated, active release of Hsp70 has been documented by several laboratories (4-7). Extracellular localized Hsp70s exert immunomodulatory capacities and play key roles in the activation of the innate immune system. Monocytes secreted proinflammatory cytokines in response to soluble Hsp70

protein through a CD14-dependent signaling pathway (8,9), and membrane-bound Hsp70 was identified as a target structure for the cytolytic attack mediated by natural killer (NK) cells. By using autologous tumor sublines with differential Hsp70 membrane expression pattern (10), we showed that Hsp70 high-expressing tumor cells are killed significantly better by NK cells as compared with their low-expressing counterparts (2,10). In addition, incubation of NK cells with soluble Hsp70 protein or with Hsp70 peptide TKD plus low-dose interleukin-2 (IL-2) further enhanced the cytolytic activity of NK cells and initiated the secretion of IFN-γ (11). In contrast, CD3^{+} T lymphocytes did not respond to an identical stimulation (12).

It was known that members of the HSP70 family act most efficiently if they operate in concert with other cochaperones that dictate their function in distinct cellular compartments (13,14). Members of the antiapoptotic Bcl-2–associated athanogene (BAG) family are frequently associated with members of the HSP70 family. Bag-4, also termed as "silencer of death domain," was found to interact with Hsp70 not only in the cytosol but also on the plasma membrane (15). Regarding these results, we asked the question whether Hsp70 and Bag-4 were released from plasma membrane–positive tumor cells in soluble form or in membrane vesicles. Exosomes correspond to internal multivesicular bodies that are secreted upon fusion with the plasma membrane (16). Apart from professional antigen-presenting cells (APC; refs. 17-19), T cells (20), reticulocytes (21,22), platelets (23), mast cells (24,25), and also tumor cells (26, 27) have been described to release exosomes. Here, we show that Hsp70/Bag-4 was actively released from colon and pancreas tumor sublines in detergent-soluble vesicles, with biophysical characteristics of exosomes. The composition of surface-bound proteins on exosomes reflected that of the plasma membranes of the tumors from which they originated. Similar to TKD, exosomes presenting Hsp70/Bag-4 on their surface stimulated migration and lytic activity in NK cells against Hsp70 membrane-positive tumors. Our data show for the first time that tumor-derived exosomes stimulate NK cell activity.

Materials and Methods

Cell culture of carcinoma sublines

By fluorescence-activated cell sorting, human pancreas (Colo357; Centre for Applied Microbiology and Research, Salisbury, Wiltshire, United Kingdom) and colon (CX2; Tumor-zellbank, DKFZ, Heidelberg, Germany) carcinoma cells were separated into the sublines Colo−/Colo+ and CX−/CX+, using the FITC-conjugated Hsp70-specific monoclonal antibody cmHsp70.1 (Multimmune, GmbH, Regensburg, Germany). Colo− (34%) and CX− (20%) cells contained consistently low and Colo+ (73%) and CX+ (90%) tumor sublines and high percentages of Hsp70 membrane-positive cells (28,29). The *Mycoplasma*-free carcinoma sublines and K562 cells were kept under exponential growth conditions by regular cell passages in RPMI 1640 supplemented with 5% heat-inactivated FCS (both from Life Technologies, Eggenstein, Germany), 50 units/mL penicillin, 50 μg/mL streptomycin, 2 mmol/L L-glutamine, and 1 mmol/L sodium pyruvate. Plating efficiency, doubling time (20 hours), and protein content were comparable in Hsp70/Bag-4 low- and high-expressing tumor sublines under physiologic conditions.

Flow cytometry of carcinoma sublines

Single cell suspensions of viable carcinoma sublines (0.1×10^6 cells per antibody) were incubated either with a FITC-conjugated Hsp70 monoclonal antibody (cmHsp70.1, Multimmune) or Bag-4–specific antibody (IMG-152, Imgenex, San Diego, CA) for 15 minutes at 4°c. Following washing in PBS/10% heat-inactivated FCS, Bag-4–stained cells were incubated with a phycoerythrin-conjugated secondary antibody for another 15 minutes (DAKO, Glostrup, Denmark). Only viable, 7-amino-actinomycin D-negative (7-AAD, Becton

Dickinson PharMingen, Heidelberg, Germany) cells were analyzed on a FACSCalibur flow cytometer (Becton Dickinson).

Preparation of cell-free supernatants and exosome purification

Tumor sublines were grown for 72 hours in conditioned medium reaching ~80% confluence. After another 24 to 72 hours in serum-free, conditioned medium, viability of the cells was always >97% as determined by trypan blue exclusion. Following successive centrifugation at $200 \times g$ for 5 minutes and $1,000 \times g$ for 10 minutes at 4°c, supernatants were passed through 200 nm filters (Sartorius, Gottingen, Germany) and concentrated on VivaSpin concentrators with a M_r 50,000 molecular weight cutoff (Vivascience, Sartorius). Concentrated supernatants were further separated by ultracentrifugation ($150,000 \times g$, 12 hours at 4°c). Total protein amount was determined using a standard Bradford assay.

Quantification of heat shock protein 70 released by tumor sublines

Briefly, 1:1 dilutions of Colo−/Colo+ and CX−/CX+ supernatants were prepared using either PBS, Triton X-100 (1% v/v), Lubrol WX (1% v/v), or Brij 98 (0.5% v/v). After a 30-minute incubation period at 4°c under gentle rotation, the amount of Hsp70 was quantified by ELISA technique (Hsp70 EIA, Stressgen, Victoria, British Columbia, Canada). All detergents were kindly provided by Prof. Dr. Gerd Schmitz (Institute of Clinical Chemistry, University Hospital Regensburg, Regensburg, Germany). Dilution of recombinant Hsp70 protein in the detergents mentioned above did not affect the detection of Hsp70 in ELISA (data not shown).

SDS-PAGE and Western blot analysis

Whole cell lysates and exosomal pellets were solubilized in lysis buffer [120 mmol/L sodium chloride, 40 mmol/L Tris (pH 8.0), 0.5% NP40] and proteins were denatured in sample buffer [25 mmol/L Tris hydrochloride (pH 6.8), 2% SDS, 10% glycerol, 10% mercaptoethanol, bromphenol blue]. Proteins from whole cell lysates and exosomes (10 μg/lane) were separated on a 10% SDS-PAGE under reducing conditions (30) and used for silver stain (RotiBlack P kit, Roth, Karlsruhe, Germany) or blotted onto nitrocellulose membranes (31) and stained with primary antibodies directed against Bag-4 (IMG-152), Hsp70 (cmHsp70.1), and Hsc70 (SPA-820, Stressgen); Grp94 and calnexin (both from Stressgen); α-tubulin (Oncogene, San Diego, CA); and Rab-4, Rab-7, Rab-9, and Rab-11 (all from Santa Cruz, Santa Cruz, CA). Proteins were visualized using horseradish peroxidase–conjugated secondary antibodies (DAKO) and a chemiluminescence developing kit (ECL, Amersham Biosciences, Buckinghamshire, England).

Sucrose density gradient centrifugation and acetylcholinesterase activity

Exosomes were floated in a sucrose density gradient ranging from 1.08 to 1.24 g sucrose/mL in TBS (pH 7.5) and ultracentrifuged ($150,000 \times g$ for 12 hours at 4°c; ref. 19). Gradient fractions containing exosomes were collected from top to bottom and analyzed by silver stain, Western blot analysis, and tested for acetylcholinesterase activity (32). Briefly, 50 μL of each individual fraction was suspended in 1.25 mmol/L acetylthiocholine and 0.1 mmol/L 5.5-dithio-bis(2-nitrobenzoic acid) in a final volume of 1 mL. Changes in absorption were monitored at 412 nm during a 10-minute incubation period at 37°c. Data represent the increase in absorption after 10-minute incubation.

Coupling of exosomes to latex beads and flow cytometric analysis of exosome-coated beads

Exosomes (30 μg) were incubated with 4-μm-diameter aldehyde/sulfate latex beads (Interfacial Dynamics, Portland, OR) for 15 minutes at 20°c in a final volume of 100 μL (33). After a 2-hour incubation period in PBS under gentle rotation, the reaction was stopped by addition of 100 mmol/L glycine. Exosome-coated beads were washed twice in PBS/10% FCS, stained

with different antibodies directed against Hsp70 and Bag-4 (15), and analyzed on a Becton Dickinson FACSCalibur using Cell Quest Software. Only single beads were gated for fluorescence analysis. A "bead-only" control and an isotype-matched antibody control were prepared and fluorescence intensity was normalized to 1×10 fluorescence units for each antibody.

Immunoelectron microscopy of exosomes

Ultracentrifuged (150,000 $\times$ *g* for 60 minutes) PBS washed exosomal pellets of CX+ and CX − sublines were resuspended in 20 μL aqua bidest and a Formvar-coated 400-mesh nickel grid was placed on top of the suspension drop. Then, grids with adherent exosomes were fixed in 4% paraformaldehyde in PBS at 20°c for 15 minutes. The subsequent immunolabeling was carried out using the IGL-Labeling automat (Leica, Bensheim, Germany). In brief, after a 10-minute blocking in 2% normal goat serum (Aurion, Biotrend, Cologne, Germany), grids were incubated either with isotype control or Hsp70 (cmHsp70.1) mouse monoclonal antibody diluted 1:50 in 1% PBS/bovine serum albumin (BSA) solution at 20°c for 2 hours. After washing, the grids were incubated for 1 hour in 1% PBS/BSA buffer containing 1:20 dilution of the Aurion goat–anti-mouse IgG-gold conjugate (10 nm). After an additional fixation step in 2% glutaraldehyde/PBS and washing in aqua bidest, the negative staining with 1% phosphotungstic acid in water (1 minute at 20°c) was done.

Grids were examined in a LEO912AB electron microscope (Zeiss, Oberkochen, Germany) operating at 80 kV, equipped with a bottom-mounted charged coupled device camera capable to record images with 1×1 k pixels. The digital documentation and measuring was done with the EsiVision software, Version 3.2 (Soft Imaging System, Muenster, Germany).

Separation and stimulation of natural killer cells

NK cells were selected from peripheral blood mononuclear cells derived from healthy human volunteers, using either CD94-biotin antibody (clone HP3 D9, Ancell Immunology Research Products, Bayport, MN) and antibiotin magnetic microbeads for positive selection, or CD3- and CD19-antibody–coated beads for negative selection following standard protocols of Miltenyi (Bergisch Gladbach, Germany). NK cells (2×10^6 cells/mL) were stimulated either with low-dose IL-2 alone (100 IU/mL) or with low-dose IL-2 in combination with TKD (2 μg/mL; Bachem, Bubendorf, Switzerland), with exosomal protein (0.1, 1, and 10 μg/mL), or with whole cell lysates (1 and 10 μg/mL) at 37°c in a humidified atmosphere containing 5% CO_2 for 4 days. Either fresh or frozen supernatants of the 4-day cell cultures were collected and analyzed by ELISA (see below). Purity and cell surface density of different NK cell markers were determined before and on day 4 after stimulation using a CD94-phycoerythrin–specific (Ancell), CD3-FITC CD16/CD56-phycoerythrin (Becton Dickinson), NCR (NKp30, NKp44, NKp46, Beckman Coulter, Krefeld, Germany), NKG2D (R&D, Wiesbaden, Germany), CD69 (Becton Dickinson), and KIR (p58, Immunotech, Marseille, France) antibodies by flow cytometry using a standard protocol.

Migration assay

Migration assays were done in transwell cell culture systems (Costar, Corning Incorporated, Corning, NY) in triplicates as previously described (28). Either concentrated supernatant of the different tumor cells, exosome-depleted and enriched fractions, or TKD (2 μg/mL) were placed in the lower compartment as attractants. Sodium [^{51}Cr]chromate–labeled (100 μCi, NEN-Dupont, Boston, MA), TKD-stimulated, CD94^{+}, or CD3^{−}CD19^{−} NK cells (2×10^6) were used as effector cells.

For blocking experiments, TKD peptide and Colo+ derived exosomes were preincubated with the Hsp70-specific antibody cmHsp70.1 at a final concentration of 50 μg/mL for 20 minutes.

Cytotoxicity assay

CX+/CX−, Colo+/Colo−, and K562 tumor target cells (0.3×10^6) labeled with sodium [^{51}Cr] chromate (100 μCi; NEN-Dupont) were coincubated with CD94-enriched or CD3/CD19-depleted NK cells, prestimulated for 4 days either with low dose IL-2 alone (100 IU/mL), with IL-2 plus TKD (2 μg/mL), with IL-2 plus exosomes (10 μg/mL), or with IL-2 plus cell lysates (10 μg/mL) derived from Colo−/Colo+ and CX−/CX+ tumor sublines, at indicated effector-to-target (E/T) cell ratios according to a protocol of MacDonald et al. (34). For antibody blocking studies, labeled tumor target cells were incubated with cmHsp70.1 antibody (5 μg/mL) for 20 minutes. After a 4-hour incubation period at 37°C, 5% CO_2 supernatants were harvested and radioactivity was determined by γ-counting. The percentage of specific lysis was calculated according to the following equation:

$$\% \text{ specific lysis} = \frac{(\text{experimental release} - \text{spontaneous release})}{(\text{maximum release} - \text{spontaneous release})} \times 100$$

The spontaneous release was less than 15% for each target cell.

Granzyme B ELISA

Granzyme B released by effector cells during the stimulation period of 4 days, either with TKD (2 μm/mL) or different amounts of exosomes (0.1, 1, and 10 μm/mL) derived from Colo− and Colo+ cell cultures, was quantified by standard ELISA technique. Briefly, granzyme B antibody-coated (L100-114, Hoelzel Diagnostics, Cologne, Germany) 96-well plates (3590, Corning Costar) were incubated with 100 μL samples or standard solutions at different concentrations in combination with the secondary capture antibody for 2 hours at room temperature. After two washing steps, granzyme B was visualized by the addition of the freshly prepared avidin-horseradish peroxidase for 1 hour and substrate solution for another 25 minutes. Plates were counted on a ELISA reader at 450/650 nm.

Results

Pancreas and colon carcinoma sublines with differential Hsp70/Bag-4 membrane expression secrete heat shock protein 70 in detergent-soluble vesicles

Human pancreas (Colo357) and colon (CX2) carcinoma cell lines were separated in stably Hsp70 low (Colo−, CX−) and high (Colo+, CX+) membrane-expressing tumor sublines by Hsp70 antibody-based cell sorting, as described previously (28). Under physiologic conditions, 34% ± 5 of the Colo− and 20% ± 6 of the CX− tumor sublines exhibited an Hsp70 membrane-positive phenotype. In contrast, the percentage of Hsp70 membrane-positive cells was significantly higher in Colo+ (73% ± 5) and CX+ (90% ± 8) tumor cells (Table 1A). As a positive control, MHC class I expression was also determined (Table 1A). In the cytosol, Hsp70 stochiometrically binds to the conserved BAG domain of Bag-4 (35). We found that tumor sublines with differential Hsp70 plasma membrane expression pattern also differ in their Bag-4 membrane phenotype (15). The percentage of Bag-4 membrane-positive cells was consistently higher in Colo+ (78% ± 1) and CX+ (78% ± 2) tumor sublines, as compared with Colo− (29% ± 11) and CX− (42% ± 10) tumor sublines (Table 1A). Nonspecific staining could be excluded because only viable cells with intact plasma membranes were analyzed. Representative flow cytometric profiles of Hsp70 (*top*) and Bag-4 (*bottom*) on Colo−/Colo+ and CX−CX+ tumor sublines were illustrated in Fig. 1A. In contrast to the significant differences in their membrane expression pattern, cytosolic protein amounts of Hsp70/Bag-4 were comparable in whole cell lysates of Colo−/Colo+ (15) and CX−/CX+ (10) tumor sublines.

Several laboratories reported about active release of Hsp70 from tumor cells (4-6). After a 24-hour incubation period of tumor sublines Colo−/Colo+ and CX−/CX+ in serum-free medium, only low amounts of soluble Hsp70 protein (5-10 ng/mL) were detectable in the medium (Fig.

1B, *filled circles*). However, treatment of the supernatants with Triton X-100 (1% v/v), Lubrol WX (1% v/v), and Brij 98 (0.5% v/v) resulted in a significant increase in Hsp70 (Fig. 1B). No significant difference in the overall Hsp70 protein content was detectable in solubilized vesicles derived from Colo−/Colo+ and CX−/CX+ tumor sublines. These data provided a first hint that Hsp70 might be secreted in detergent-soluble vesicles.

Detergent-soluble vesicles exhibit biophysical and biochemical properties of exosomes

B lymphocytes and dendritic cells have been documented to secrete membrane vesicles of endocytic origin, termed exosomes (18,24,33). Exosomes are formed upon fusion of internal multivesicular bodies with the plasma membrane. In addition to hematopoietic cells, secretion of exosomes was also found in tumor cells (27). Following a modified protocol described by Thery et al. (18,33), 10 to 15 μg vesicular proteins were prepared from sequentially centrifuged supernatants of 1×10^7 viable Colo+ and CX+ tumor cells cultured in serum-free medium and subjected to sucrose density gradient ultracentrifugation. As shown in Fig. 2A (*top*), an enrichment of proteins was found at densities of 1.15 to 1.19 g/mL in both cell types. Acetylcholinesterase activity, a characteristic enzyme in reticulocyte-derived exosomes (32, 36), also peaked at a floating density of 1.17 g/mL (Fig. 2A, *bottom*). Identical results were obtained for Colo− and CX− tumor sublines, indicating that these tumor sublines also had the capacity to release exosomal vesicles (data not shown). Taken together, these results suggested that vesicles obtained from cell-free supernatants of tumor cells exhibited biophysical properties of exosomes (18). Contamination of the exosomal fraction with apoptotic bodies was excluded for the following reasons: (*a*) viability of tumor sublines from which the supernatants were collected was always greater 97%; therefore, nonspecific release of membrane vesicles by dead cells was unlikely; (*b*) apoptotic vesicles exhibit a characteristic molecular weight histone protein pattern, which was not visible in the vesicular preparations, and float at higher densities, ranging from 1.24 to 1.28 g/mL (18); (*c*) tumor-derived exosomes float at a characteristic density of 1.17 g/mL (24,27,33); (*d*) acetylcholinesterase activity, an exosomal enzyme, peaked at the same density of 1.17 g/mL.

A comparison of the protein profiles of whole cell lysates and exosomes revealed that lysates of all tumor sublines were very similar albeit clearly distinct form that of exosomes (Fig. 2B, *top*). Western blot analysis indicated that cytosolic proteins, including tubulin, Bag-4, Hsp70, and Hsc70, were found in both whole cell lysates and exosomes, whereas endoplasmic reticulum–residing proteins, including Grp94 and calnexin, were absent in exosomes (Fig. 2B, *bottom*). Consistently, the small GTPase Rab-4 (early endosome to plasma membrane) was found to be highly enriched in exosomes; weak amounts of Rab-11 (*trans*-Golgi to plasma membrane) were detectable. Rab-7 (late endosome to lysosome) and Rab-9 (late endosome to *trans*-Golgi) were absent in exosomes. Regarding these results, we hypothesized that tumor-derived exosomes originate from early endosomes.

Surface protein pattern of exosomes reflects that of the tumor sublines from which they originated

Identical to the cytosol, the exosomal lumen contained comparable protein amounts of Hsp70 and Bag-4, irrespective of the tumors from which they originated (15). However, on the plasma membrane, these proteins were differentially expressed on Colo−/Colo+ and CX−/CX+ sublines. Due to the fact that exosomes are formed by inward budding of endosomal membranes, exosomal surfaces should reflect the protein composition of the plasma membranes of the cells from which they were derived. This was also shown for MHC class I/II, tetraspan, and costimulatory molecules (18,33,37). Because of their biogenesis, the topology of exosomal proteins should also remain the same. Therefore, we compared the Hsp70/Bag-4 surface expression pattern on the plasma membrane of tumor cells (Fig. 1A) and exosomes. A representative flow cytometric analysis revealed high Hsp70/Bag-4 levels selectively on the

exosomal surface of Colo+ and CX+ tumor sublines (Fig. 2C). Consistent with a low Hsp70/Bag-4 plasma membrane expression on Colo− and CX− tumor sublines (Fig. 1A), exosomes derived from these cells were also weakly surface-positive for Hsp70/Bag-4 (Fig. 2C). Flow cytometry data of exosomes derived from three independent experiments were summarized in Table 1B. It is important to note that only antibodies cmHsp70.1 and IMG-152 detected membrane-bound Hsp70/Bag-4 on the exosomal surface and on the plasma membrane of viable tumors. Antibodies directed toward the NH$_2$-terminal domains of Hsp70 and Bag-4 (15) failed to do so (data not shown). These data indicated that the topology of both molecules on the plasma membrane and on the exosomal surface was identical. Irrespective of their origin, exosomes were strongly positive for MHC class I (Table 1B). Localization of Hsp70 was also documented by immunoelectronmicroscopy on the exosomal surface of CX+ cells (Fig. 2D, *bottom*). It seemed that Hsp70 is frequently found in pairs on the exosomal surface of CX+ cells. In contrast, exosomes derived from CX− cells completely lack Hsp70 on their surface (Fig. 2D, *top*). No staining was detected on exosomes stained with control antibody (data not shown). Taken together, our results indicated that despite an identical Hsp70/Bag-4 content in the exosomal lumen, the surface of exosomes reflected that of the tumor cell membranes from which they originated.

Hsp70/Bag-4 surface-positive exosomes induce specific migration in TKD-activated natural killer cells

The C-type lectin receptor CD94 was found to be involved in the interaction of NK cells with Hsp70 protein and also with the 14-mer Hsp70 peptide TKDNNLLGRFELSG (aa$_{450-464}$, TKD; ref. 38). Recently, we have shown that CD94$^+$ NK cells, but not CD3$^+$ T lymphocytes, specifically migrated toward Hsp70 membrane-positive tumor cells (Colo+ and CX+) and culture supernatants derived thereof (28). These findings indicated that a soluble factor released by Hsp70 membrane-positive tumor cells might initiate migration. Indeed, full-length Hsp70 protein and TKD both induced specific chemotaxis in a dose-dependent manner (28). Here, we examined exosomes with high and low Hsp70/Bag-4 surface expression as attractants for NK cells. Stimulation of NK cells with TKD for 4 days was a prerequisite for their migratory capacity. Preactivated, CD94$^+$ NK cells were placed in the upper compartment of the transwell system; the lower compartment was loaded either with 2-fold concentrated, cell-free supernatants (SN*) of the tumor sublines Colo /Colo+ and CX /CX+, as controls, or with exosome-depleted or exosome-enriched fractions of the identical tumor sublines (Fig. 3A). NK cells migrated toward cell culture supernatants (SN*) of Hsp70/Bag-4 membrane-positive Colo + (18%) and CX+ (12%) tumor cells (*black columns*) but not toward supernatants of Hsp70/Bag-4–negative Colo− (7%) and CX− (4%) tumor cells (*white columns*). These results corroborated previous findings from our group (28). Irrespective of their origin, exosome-depleted fractions lack any chemotactic activity. In contrast, exosome-enriched fractions of Colo+ (24%) and CX+ (15%) supernatants initiated a strong chemotactic activity in NK cells, whereas exosome-enriched fractions derived from Colo− (7%) and CX− (3%) cells failed to do so. As an internal control, migration of NK cells was also tested against TKD (Fig. 3B). In line with previous results, CD94$^+$ NK cells migrated toward TKD (14%). This migratory capacity was inhibited by Hsp70–specific antibody (cmHsp70.1), whose epitope is part of the TKD sequence, as indicated in bold: TKDN**NLLGRFELSG** (39). The marked reduction in the percentage of migrating NK cells from 14% to 4% is illustrated in Fig. 3B (*left*). An MHC class I–specific antibody (W6/32) had no inhibitory capacity on NK cell migration toward TKD. Comparable results were obtained if exosomes derived from Colo+ cells were used as an attractant. Initial migratory capacity of NK cells toward Colo+ exosomes was 17%; the Hsp70–specific antibody reduced the migratory capacity to 3%, indicating that, indeed, Hsp70 presented on the surface of exosomes was responsible for the migratory capacity of NK cells. Although tumor-derived exosomes were found to be MHC class I surface positive, the

migratory capacity of NK cells was not negatively affected by preincubation of the exosomes with an MHC class I–specific antibody (W6/32).

Hsp70/Bag-4 membrane-positive exosomes boost cytolytic function cells through granzyme B release concomitant with an enhanced cell surface density of several natural killer cell receptors

Hsp70/Bag-4 high-expressing Colo+ and CX+ tumor cells were susceptible to the cytolytic attack mediated by CD94^{+} NK cells after stimulation with low-dose IL-2 plus TKD (10,11, 40). In contrast, T cells did not respond to this stimulus (12). Because Hsp70/Bag-4 surface-positive exosomes initiated migration in CD94^{+} NK cells, we examined their immunomodulatory capacity. Therefore, purified CD94^{+} or CD3^{−} CD19^{−} NK cells were incubated either with exosomes derived from Hsp70/Bag-4 low-expressing Colo− and CX− cells. or from high-expressing Colo+ and CX+ tumor As controls, NK cells were activated either with low dose IL-2 plus TKD, or with low dose IL-2 alone (control). Stimulation with TKD resulted in a significantly enhanced cytolytic activity of NK cells against the Hsp70/Bag-4–positive Colo+ and CX+ tumor cells, if compared with their Hsp70/Bag-4 low-expressing counterparts Colo− and CX− (Fig. 4A, *left*). NK cells cultivated in the presence of 10 A μg/mL Hsp70/Bag-4–negative exosomes (Colo− exos) plus low dose IL-2 showed a weaker lytic activity toward both target cell types, and differences in lysis of Hsp70/Bag-4 low- and high-expressing tumor target cells was less pronounced (Fig. 4A, *right*). These data suggested that Colo− and CX− derived exosomes did not specifically induce Hsp70-reactivity. In contrast, NK cells stimulated with Hsp70/Bag-4–positive exosomes (10 μg/mL) plus low dose IL-2 exhibited a strong lytic capacity toward Hsp70 membrane-positive tumor target cells Colo+ and CX+ and K562 cells (Table 2A). A concentration of 0.1 and 1 μg/mL exosomes was insufficient to activate NK cells (data not shown). Differences in the lysis of Hsp70/Bag-4–positive and Hsp70/Bag-4–negative tumor target cells were comparable with that obtained with TKD-activated NK cells. Statistically significant differences in the lytic activity of differentially activated CD3^{−}CD19^{−} NK cells against Colo−/Colo+, CX−/CX+, and K562 tumor target cells are summarized in Table 2A. As a control, tumor cell lysates of CX+/CX− cells in combination with low dose IL-2 were used. Differences in lysis of Hsp70 membrane-positive and membrane-negative tumor cells were not observed after this stimulation (Table 2A). The increased lysis of Hsp70 surface-positive CX+ and K562 tumor cells by NK cells preactivated either with TKD or exosomes derived from CX+ but not of CX− tumor cells was blockable by Hsp70-specific antibody cmHsp70.1. Taken together, these results indicated that similar to TKD, Hsp70/Bag-4–positive exosomes are highly efficient in stimulating Hsp70 reactivity in NK cells.

NK cells activated with exosomes of Colo+ tumor cells showed good lysis of autologous Colo+ tumor cells but weaker lysis of Colo− tumor cells (Fig. 4A). Interestingly, a similar lysis pattern was detectable if allogeneic CX+ tumor cells were used as target cells (Fig. 4B). These data showed that Hsp70 reactivity is generally induced by Hsp70/Bag-4 surface-positive exosomes irrespective of their tumor cell origin. Mean values of three independent experiments are summarized in Table 2B.

Previous work indicated that the lytic activity against Hsp70/Bag-4 membrane-positive tumor cells was mediated through the apoptosis-inducing protease granzyme B (41), which provides a surrogate marker for the lytic potential of NK cells. Therefore, cell culture supernatants of NK cells were collected and analyzed quantitatively for the presence of granzyme B after a stimulation period of 4 days with either IL-2 alone or with IL-2 plus different amounts of exosomes derived from Colo− and Colo+ tumor cells. As shown in Fig. 4C, significant release of granzyme B was induced when NK cells were stimulated with 10 μg/mL Hsp70/Bag-4–positive Colo+ exosomes (73 ng/mL). Identical amounts of Hsp70/Bag-4 low-expressing Colo

− exosomes resulted in a significantly weaker release of granzyme B (38 ng/mL). Only 17 ng/ mL granzyme B was released if NK cells were stimulated with IL-2 alone. Similar results were obtained with exosomes derived from CX+/CX− tumor cells (data not shown). Concomitantly, the cell surface density of CD94, CD56, and CD69 was significantly up-regulated after incubation of NK cells either with TKD or Hsp70/Bag-4 surface-positive exosomes; that of NCRs NKp30, and NKp44 was enhanced by any of the tested stimuli (Table 2C). No significant increase in the cell surface density was observed with respect to NKp46 and NKG2D; that of CD158 was even down-regulated. It is worth mentioning that following stimulation with TKD and Hsp70/Bag-4 surface-positive exosomes, the percentage of NKp30 (46% ± 14), NKp44 (23% ± 12), and CD69 (21% ± 8) positive cells remained significantly lower than that of CD94, NKG2D, and NKp46 (always above 85%).

Discussion

Hsp70 is a major player in protein transport across membranes (1). In the cytosol, Bag-4, also termed as silencer of death domain, binds to the ATPase domain of Hsp70 (42). Therefore, it was conceivable that Hsp70 in concert with Bag-4 might fulfill shuttle functions from inside the cell to the plasma membrane. Indeed, Hsp70 was found to be associated with Bag-4 on the plasma membrane of Colo+ pancreas and CX+ colon carcinoma sublines, as compared with their low-expressing counterparts Colo− and CX− (15). Despite these differences in the cell surface pattern, no interindividual differences were observed with respect to their cytosolic Hsp70/Bag-4 content, thus indicating that translocation to the plasma membrane might be independent from *de novo* protein synthesis.

Although the mechanism of transport remained elusive, several groups reported about release of Hsp70 from viable tumor cells that could be further enhanced by exogenous stress (4-6). Recently, an alternative vesicular pathway of Hsp70 export from colon carcinoma cells was hypothesized, not involving the endoplasmic reticulum-Golgi compartment (5). These findings are in line with our unpublished observations that drugs perturbing endoplasmic reticulum-Golgi transport, including monensin and brefeldin A, neither affected plasma membrane expression nor export of Hsp70.[4]

Here, we addressed the question whether differences in the Hsp70/Bag-4 membrane expression pattern were associated with a different capacity to export these molecules. We found that spontaneous release of soluble Hsp70 by both tumor sublines was rather low. In contrast, detergent-soluble vesicles actively released by both tumor cell types contained high amounts of Hsp70/Bag-4. Biochemical and physical characteristics identified them as exosomes corresponding to internal vesicles, produced by inward budding of endosomal membranes in a process sequestering particular proteins and lipids (16). An enrichment of Rab-4 in exosomes documented their intracellular transport route from early endosomes to the plasma membrane. With respect to their biogenesis, exosomal surfaces resembled that of the plasma membranes from the tumor sublines from which they originated. Even the topology of Hsp70 in the exosomal surface remained identical because only antibodies directed against the COOH terminus reacted with surface-bound molecules.

A recent study highlighted the presence of lipid raft micro-domains in exosomal membranes and suggested their participation in vesicular formation (26). In collaboration with the group of Alexzander Asea, we provided evidence that lipid rafts are indeed involved in stress-induced export of Hsp70 by erythroleukemic K562 cells.[4] With respect to their function, different possibilities are presently hypothesized. During reticulocyte maturation, secretion of exosomes

---

[4]M.A. Bausero et al. Alternative mechanism by which IFN-γ enhances tumor recognition: active release of Hsp72. J Immunol, submitted for publication.

was found to be associated with loss of the transferrin receptor together with Hsc70. It was assumed that this release enables reticulocytes to externalize obsolete proteins (43). On the other hand, APC-derived exosomes were enriched in immunostimulatory molecules, including MHC class I/II molecules, Hsp70, and Hsc70 (17,24). This led us to the hypothesis that our tumor-derived exosomes play a major role in the intracellular communication of the immune system. Tumor-derived exosomes provide a source for shared tumor rejection antigens for cross-priming (27). We have shown that contact of NK cells with soluble Hsp70 protein and TKD resulted in an increased cytolytic activity against Hsp70 membrane-positive tumor cells and initiated specific migration (11,28,29). Here, we showed that selective exosomes generated from supernatants of Hsp70/Bag-4–positive pancreas (Colo+) and colon (CX+) carcinoma sublines induced migration and cytolytic activity in NK cells that could be completely abrogated by Hsp70-specific antibody. Similar to TKD, exosome-stimulated NK cells kill their targets via granzyme B–mediated apoptosis (41).

It was known from other studies that exosomes derived from APCs have the capacity to prime naive CD8^{+} T lymphocytes to eradicate tumors (17). Here, we show for the first time that exosomes originating from Hsp70/Bag-4 membrane-positive tumor cells stimulate migration and Hsp70 reactivity in NK cells. In conclusion, depending on their cellular origin, exosomes might be considered as intercellular transporters, trafficking differential stimulation between the adaptive and innate immune system.

References

1. Hartl FU, Hayer-Hartl M. Molecular chaperones in the cytosol: from nascent chain to folded protein. Science 2002;295:1852–8. [PubMed: 11884745]
2. Multhoff G, Botzler C, Wiesnet M, et al. A stress-inducible 72-kDa heat-shock protein (HSP72) is expressed on the surface of human tumor cells, but not on normal cells. Int J Cancer 1995;61:272–9. [PubMed: 7705958]
3. Shin BK, Wang H, Yim AM, et al. Global profiling of the cell surface proteome of cancer cells uncovers an abundance of proteins with chaperone function. J Biol Chem 2003;278:7607–16. [PubMed: 12493773]
4. Barreto A, Gonzalez JM, Kabingu E, Asea A, Fiorentino S. Stress-induced release of HSC70 from human tumors. Cell Immunol 2003;222:97–104. [PubMed: 12826079]
5. Broquet AH, Thomas G, Masliah J, Trugnan G, Bachelet M. Expression of the molecular chaperone Hsp70 in detergent-resistant microdomains correlates with its membrane delivery and release. J Biol Chem 2003;278:21601–6. [PubMed: 12682040]
6. Guzhova I, Kislyakova K, Moskaliova O, et al. *In vitro* studies show that Hsp70 can be released by glia and that exogenous Hsp70 can enhance neuronal stress tolerance. Brain Res 2001;914:66–73. [PubMed: 11578598]
7. Altmeyer A, Maki RG, Feldweg AM, et al. Tumor-specific cell surface expression of the-KDEL containing, endoplasmic reticular heat shock protein gp96. Int J Cancer 1996;69:340–9. [PubMed: 8797880]

8. Asea A, Kraeft SK, Kurt-Jones EA, et al. HSP70 stimulates cytokine production through a CD14-dependant pathway, demonstrating its dual role as a chaperone and cytokine. Nat Med 2000;6:435–42. [PubMed: 10742151]

9. Asea A, Rehli M, Kabingu E, et al. Novel signal transduction pathway utilized by extracellular HSP70: role of TLR2 and TLR4. J Biol Chem 2002;277:15028–34. [PubMed: 11836257]

10. Multhoff G, Botzler C, Jennen L, Schmidt J, Ellwart J, Issels R. Heat shock protein 72 on tumor cells: a recognition structure for natural killer cells. J Immunol 1997;158:4341–50. [PubMed: 9126997]

11. Multhoff G, Mizzen L, Winchester CC, et al. Heat shock protein 70 (Hsp70) stimulates proliferation and cytolytic activity of natural killer cells. Exp Hematol 1999;27:1627–36. [PubMed: 10560910]

12. Multhoff G, Botzler C, Wiesnet M, Eissner G, Issels R. CD3-large granular lymphocytes recognize a heat-inducible immunogenic determinant associated with the 72-kD heat shock protein on human sarcoma cells. Blood 1995;86:1374–82. [PubMed: 7632945]

13. Bukau B, Horwich AL. The Hsp70 and Hsp60 chaperone machines. Cell 1998;92:351–66. [PubMed: 9476895]

14. Hartl FU. Molecular chaperones in cellular protein folding. Nature 1996;381:571–9. [PubMed: 8637592]

15. Gehrmann M, Marienhagen J, Eichholtz-Wirth H, et al. Dual function of membrane-bound heat shock protein 70 (Hsp70), Bag-4, and Hsp40: protection against radiation-induced effects and target structure for natural killer (NK) cells. Cell Death Differ 2005;12:38–51. [PubMed: 15592361]

16. Stoorvogel W, Kleijmeer MJ, Geuze HJ, Raposo G. The biogenesis and functions of exosomes. Traffic 2002;3:321–30. [PubMed: 11967126]

17. Zitvogel L, Regnault A, Lozier A, et al. Eradication of established murine tumors using a novel cell-free vaccine: dendritic cell-derived exosomes. Nat Med 1998;4:594–600. [PubMed: 9585234]

18. Thery C, Boussac M, Veron P, et al. Proteomic analysis of dendritic cell-derived exosomes: a secreted subcellular compartment distinct from apoptotic vesicles. J Immunol 2001;166:7309–18. [PubMed: 11390481]

19. Wubbolts R, Leckie RS, Veenhuizen PT, et al. Proteomic and biochemical analyses of human B cell-derived exosomes. Potential implications for their function and multivesicular body formation. J Biol Chem 2003;278:10963–72. [PubMed: 12519789]

20. Denzer K, Kleijmeer MJ, Heijnen HF, Stoorvogel W, Geuze HJ. Exosome: from internal vesicle of the multivesicular body to intercellular signaling device. J Cell Sci 2000;113(Pt 19):3365–74. [PubMed: 10984428]

21. Dardalhon V, Geminard C, Reggio H, Vidal M, Sainte-Marie J. Fractionation analysis of the endosomal compartment during rat reticulocyte maturation. Cell Biol Int 2002;26:669–78. [PubMed: 12175670]

22. Johnstone RM. Cleavage of the transferrin receptor by human granulocytes: differential proteolysis of the exosome-bound TFR. J Cell Physiol 1996;168:333–45. [PubMed: 8707869]

23. Heijnen HF, Schiel AE, Fijnheer R, Geuze HJ, Sixma JJ. Activated platelets release two types of membrane vesicles: microvesicles by surface shedding and exosomes derived from exocytosis of multivesicular bodies and α-granules. Blood 1999;94:3791–9. [PubMed: 10572093]

24. Raposo G, Nijman HW, Stoorvogel W, et al. B lymphocytes secrete antigen-presenting vesicles. J Exp Med 1996;183:1161–72. [PubMed: 8642258]

25. Skokos D, Botros HG, Demeure C, et al. Mast cell-derived exosomes induce phenotypic and functional maturation of dendritic cells and elicit specific immune responses *in vivo*. J Immunol 2003;170:3037–45. [PubMed: 12626558]

26. De Gassart A, Geminard C, Fevrier B, Raposo G, Vidal M. Lipid raft-associated proteins are sorted in exosomes. Blood 2003;102:4336–44. [PubMed: 12881314]

27. Wolfers J, Lozier A, Raposo G, et al. Tumor-derived exosomes are a source of shared tumor rejection antigens for CTL cross-priming. Nat Med 2001;7:297–303. [PubMed: 11231627]

28. Gastpar R, Gross C, Rossbacher L, Ellwart J, Riegger J, Multhoff G. The cell surface-localized heat shock protein 70 epitope TKD induces migration and cytolytic activity selectively in human NK cells. J Immunol 2004;172:972–80. [PubMed: 14707070]

29. Multhoff G, Pfister K, Gehrmann M, et al. A 14-mer Hsp70 peptide stimulates natural killer (NK) cell activity. Cell Stress Chaperones 2001;6:337–44. [PubMed: 11795470]

30. Laemmli UK. Cleavage of structural proteins during the assembly of the head of bacteriophage T4. Nature 1970;227:680–5. [PubMed: 5432063]

31. Towbin H, Staehelin T, Gordon J. Electrophoretic transfer of proteins from polyacrylamide gels to nitrocellulose sheets: procedure and some applications. Proc Natl Acad Sci U S A 1979;76:4350–4. [PubMed: 388439]

32. Savina A, Furlan M, Vidal M, Colombo MI. Exosome release is regulated by a calcium-dependent mechanism in K562 cells. J Biol Chem 2003;278:20083–90. [PubMed: 12639953]

33. Thery C, Regnault A, Garin J, et al. Molecular characterization of dendritic cell-derived exosomes. Selective accumulation of the heat shock protein hsc73. J Cell Biol 1999;147:599–610. [PubMed: 10545503]

34. MacDonald HR, Engers HD, Cerottini JC, Brunner KT. Generation of cytotoxic T lymphocytes *in vitro*. II. Effect of repeated exposure to alloantigens on the cytotoxic activity of long-term mixed leukocyte cultures. J Exp Med 1974;140:718–30. [PubMed: 4278109]

35. Gehrmann M, Marienhagen J, Eichholtz-Wirth H, et al. Dual function of membrane-bound heat shock protein 70 (Hsp70), Bag-4, and Hsp40: protection against radiation-induced effects and target structure for natural killer cells. Cell Death Differ 2005;12:38–51. [PubMed: 15592361]

36. Johnstone RM, Bianchini A, Teng K. Reticulocyte maturation and exosome release: transferrin receptor containing exosomes shows multiple plasma membrane functions. Blood 1989;74:1844–51. [PubMed: 2790208]

37. Escola JM, Kleijmeer MJ, Stoorvogel W, Griffith JM, Yoshie O, Geuze HJ. Selective enrichment of tetraspan proteins on the internal vesicles of multivesicular endosomes and on exosomes secreted by human B-lymphocytes. J Biol Chem 1998;273:20121–7. [PubMed: 9685355]

38. Botzler C, Li G, Issels RD, Multhoff G. Definition of extracellular localized epitopes of Hsp70 involved in an NK immune response. Cell Stress Chaperones 1998;3:6–11. [PubMed: 9585177]

39. Multhoff G, Pfister K, Gehrmann M, et al. A 14-mer Hsp70 peptide stimulates natural killer (NK) cell activity. Cell Stress Chaperones 2001;6:337–44. [PubMed: 11795470]

40. Gross C, Hansch D, Gastpar R, Multhoff G. Interaction of heat shock protein 70 peptide with NK cells involves the NK receptor CD94. Biol Chem 2003;384:267–79. [PubMed: 12675520]

41. Gross C, Koelch W, DeMaio A, Arispe N, Multhoff G. Cell surface-bound heat shock protein 70 (Hsp70) mediates perforin-independent apoptosis by specific binding and uptake of granzyme B. J Biol Chem 2003;278:41173–81. [PubMed: 12874291]

42. Takayama S, Xie Z, Reed JC. An evolutionarily conserved family of Hsp70/Hsc70 molecular chaperone regulators. J Biol Chem 1999;274:781–6. [PubMed: 9873016]

43. Johnstone RM, Mathew A, Mason AB, Teng K. Exosome formation during maturation of mammalian and avian reticulocytes: evidence that exosome release is a major route for externalization of obsolete membrane proteins. J Cell Physiol 1991;147:27–36. [PubMed: 2037622]
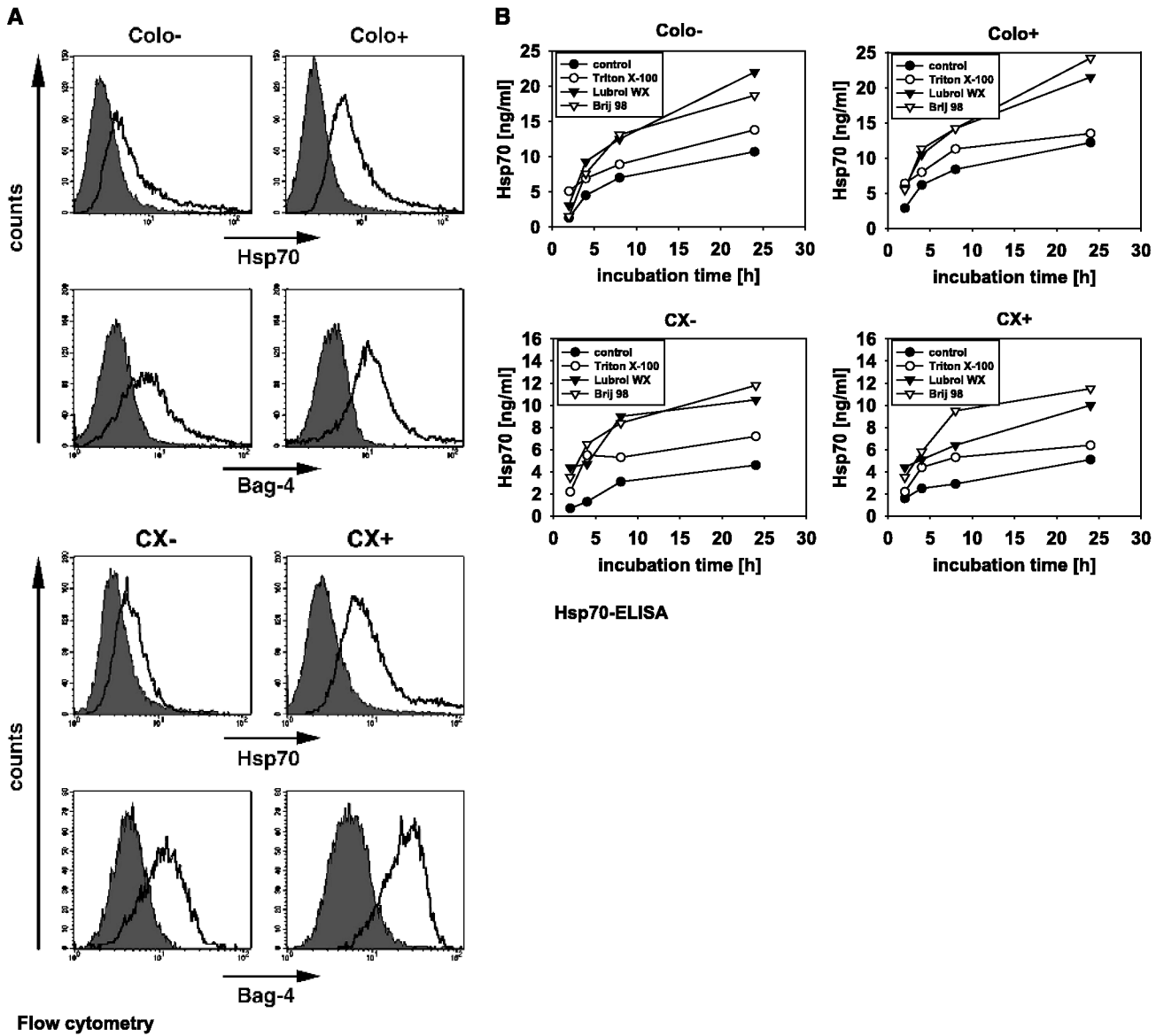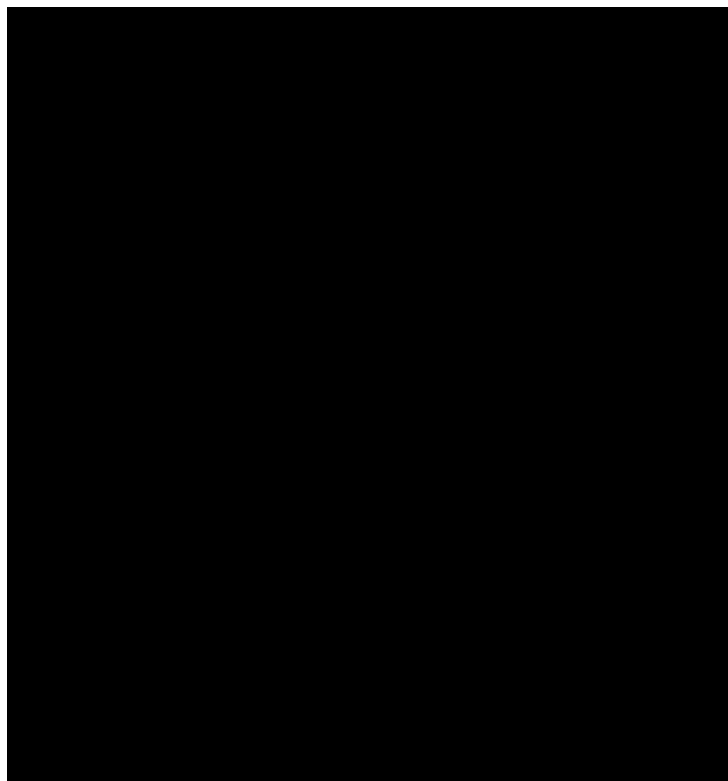
Figure 1.
A, expression of Hsp70 and Bag-4 on the plasma membrane of human pancreas (*Colo−/Colo+*) and colon (*CX−/CX+*) carcinoma sublines. Nonpermeabilized, 7-AAD negatively gated, viable carcinoma sublines Colo−/Colo+ and CX−/CX+ with intact plasma membrane were stained either with Hsp70− (cmHsp70.1) or Bag-4 (IMG-152) specific antibodies and analyzed by flow cytometry. The histograms represent positively stained cells in white, corrected for nonspecific staining, using an isotype-matched control antibody marked in gray. Mean values ± SE of three independent were summarized in Table 1A. *B*, Hsp70 and Bag-4 were actively released in detergent-soluble vesicles by viable carcinoma sublines. The amount of Hsp70 protein released by tumor sublines Colo−/Colo+ and CX−/CX+ was quantified by ELISA. Cell-free supernatants of Colo×/Colo+ (*top*) and CX−/CX+ (*bottom*) cells, diluted either in PBS buffer (control, ●), or in buffer containing the detergent Triton X-100 (1% v/v, o), Lubrol WX (1% v/v, △), and Brij 98 (0.5% v/v, ▲) were analyzed. One representative kinetic of three independent experiments was illustrated.
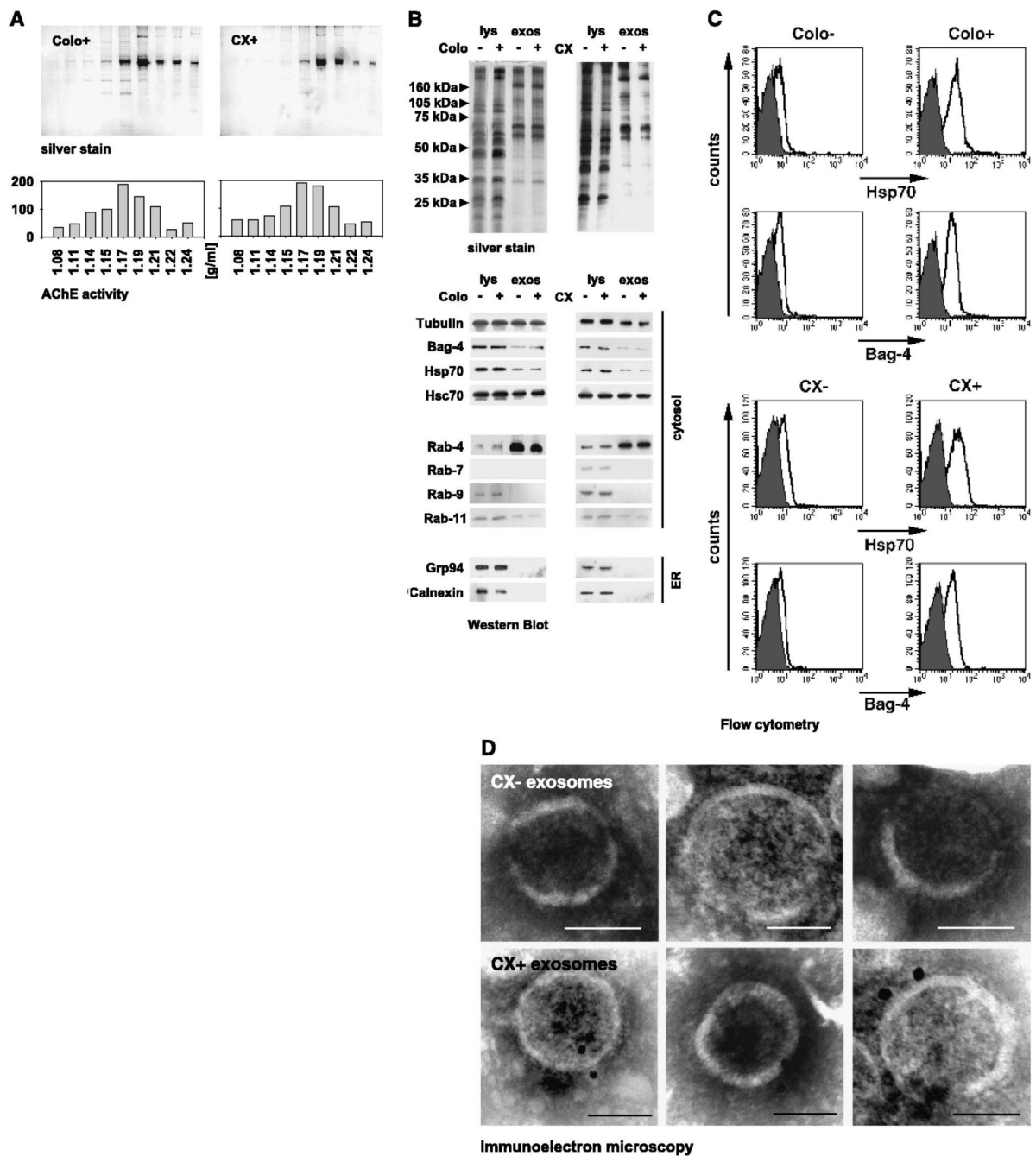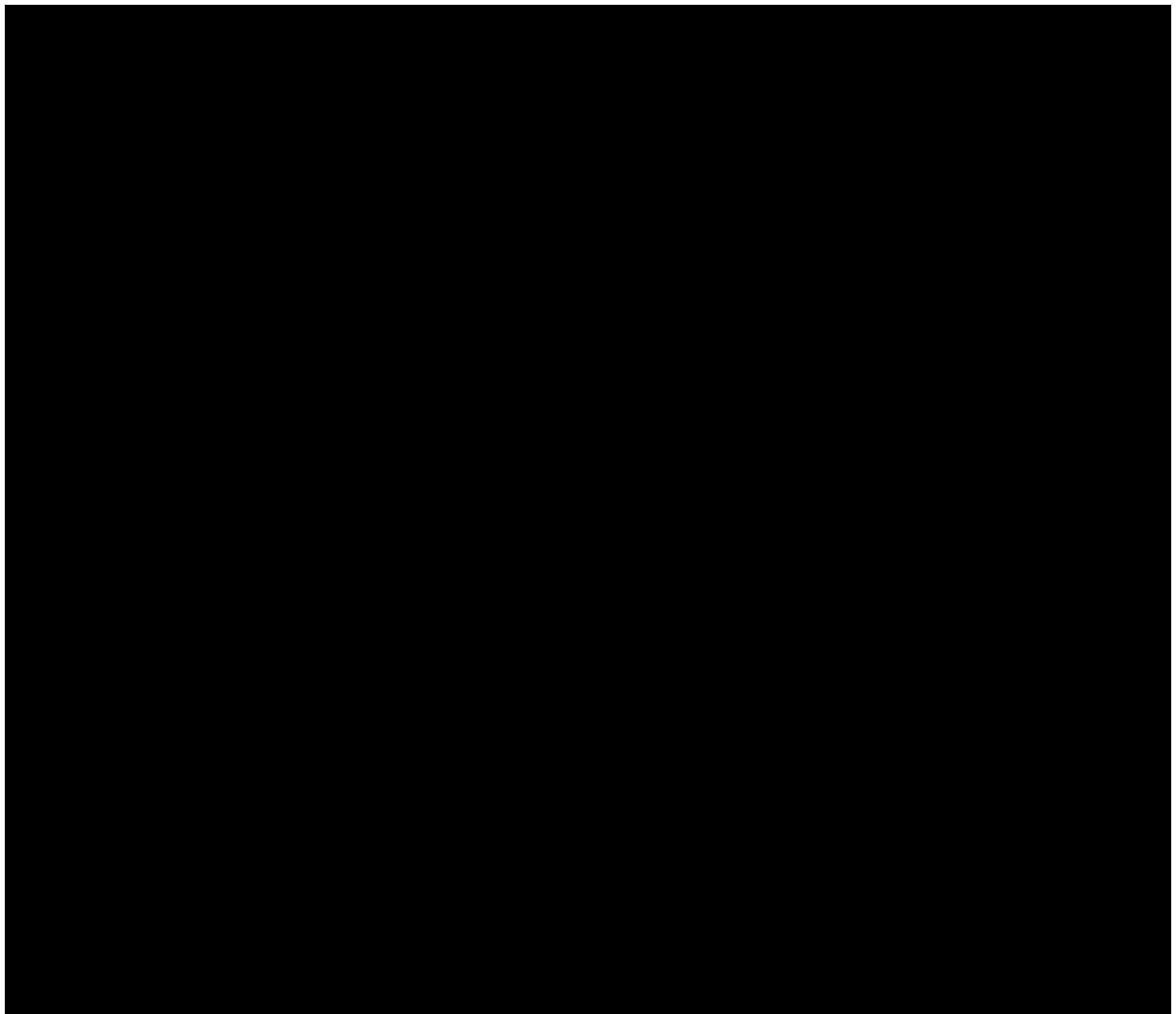
Figure 2.

A, biophysical characterization of vesicles released by Colo−/Colo+ and CX−/CX+ carcinoma sublines. Sucrose density gradient centrifugation of Colo+ (*left*) and CX+ (*right*) derived vesicles was done on a sucrose density gradient by ultracentrifugation in a density range of 1.08 to 1.24 g/mL. Fractions were collected from top to bottom and analyzed after separation on a 10% SDS-PAGE by silver stain (*top*). As a marker for exosomes, acetylcholinesterase activity was measured in each individual fraction by standard colorimetric assay. Maximum protein amount and acetylcholinesterase activity were detected at a density of 1.17 g/mL. One representative experiment of three was shown. *B*, biochemical characterization of exosomes released by Colo−/Colo+ and CX−/CX+ carcinoma sublines. Comparative analysis of the

protein composition in whole cell lysates (*lys*) and exosomal (*exos*) fractions of tumor sublines Colo−/Colo+ and CX−/CX+, as determined by silver staining (*top*) and Western blot analysis (*bottom*), using specific antibodies directed against tubulin, Bag-4, Hsp70, Hsc70, Rab-4, Rab-7, Rab-9, Rab-11, Grp94, and Calnexin. One representative silver stain and Western blot out of five was shown. *C*, surface of exosomes derived from Colo+ and CX+ carcinoma sublines are strongly positive for Hsp70/Bag-4. Exosomes derived from Colo−/Colo+ (*left*) and CX−/CX+ (*right*) carcinoma sublines were covalently bound to aldehyde/sulfate latex beads with a diameter of 4 μm. Exosome-coated beads were stained with antibodies directed against Hsp70 (cmHsp70.1, *top, white histograms*), Bag-4 (IMG-152, *bottom, white histograms*), and isotype-matched control antibodies (*gray histograms*) and analyzed by flow cytometry. Only the population containing single beads was gated and analyzed. Mean values of three independent experiments ± SE were summarized in Table 1B. *D*, immunoelectron microscopic view of the Hsp70 localization on the exosomal surface of CX− (*top*) and CX+ (*bottom*) cells at a magnification of ∼ ×60.000; scale bar, 50 nm. Localization of Hsp70 was visualized by 10 nm gold particles. No staining was found on exosomes incubated with an isotype-matched negative control antibody (data not shown).

Figure 3.
CD94^{+} NK cells specifically migrate toward Hsp70/Bag-4–positive exosomes derived from Colo+ and CX+ carcinoma sublines. *A*, VivaSpin treated (2-fold concentrated) supernatants (SN*) collected after a 24-hour cultivation period in serum-free medium, derived from Colo −/Colo+ (left) and CX−/CX+ (*right*) carcinoma sublines were used as positive controls for the migratory capacity of CD94^{+} NK cells. Exosome-depleted and exosome-enriched fractions derived from the same supernatants by ultracentrifugation at $150,000 \times g$ were also used as attractants for NK cells. The transwell system consisted of two compartments separated by a polycarbonate membrane with a pore size of 5 μm. The different attractants, unseparated supernatant (*SN*), exosome-depleted, and exosome-enriched fractions were placed in the lower compartment in a total volume of 600 μL; 0.5×10^6 ^{51}Cr-labeled CD94^{+} NK cells were placed in the upper compartment. After a 4-hour coincubation period at 37°C, the percentage of specifically migrating cells was determined in a γ-counter. B, migratory capacity of CD94^{+} NK cells was also tested toward Hsp70 peptide TKD (*right*) and exosomes derived from Colo+ carcinoma cells (*left*) either untreated or after preincubation with an MHC class I–specific (*W6/32*) or with an Hsp70-specific (*cmHsp70.1*) antibody. NK cells migrated specifically toward TKD and exosomes derived from Colo+ carcinoma cells. The MHC class I–specific antibody W6/32 did not affect migratory capacity; however, the Hsp70-specific antibody completely abrogated migratory capacity of NK cells toward TKD and Colo+ exosomes. *Columns*, mean of three independent experiments; *bars*, SE.

Figure 4.
Hsp70/Bag-4–positive exosomes derived from Colo+ and CX+ carcinoma sublines stimulate cytolytic activity of CD94^{+} NK cells against Hsp70/Bag-4–positive tumor targets. CD94^{+} NK cells were incubated either with IL-2 alone (*control*), with IL-2 plus TKD (*TKD*), or with IL-2 plus exosomes (10 μg protein/mL) derived from Colo−/Colo+ or CX−/CX+ carcinoma sublines for 4 days. *A*, cytolytic activity was measured using Colo+/Colo− and CX+/CX− carcinoma sublines as target cells in a standard ^{51}Cr release assay. A comparable, strong lysis was detected against Colo+ and CX+ carcinoma sublines if NK cells were stimulated either with IL-2 plus TKD (*TKD*) or with exosomes derived from Colo+ and CX+ carcinoma sublines. After stimulation with IL-2 alone or with exosomes derived from Colo− and CX− carcinoma sublines, lytic activity of Hsp70/Bag-4–positive tumor target cells was weaker. Mean values of three to four independent experiments ± SE, at one distinct E/T ratio of 10:1, were summarized in Table 2A. *B*, lytic activity of CD94^{+} NK cells against CX+/CX− tumor target cells was also measured after stimulation with exosomes derived from Colo−/Colo+ carcinoma sublines. Again, lysis of CX+ tumor targets was significantly enhanced by stimulation with exosomes derived from Colo+ but not of Colo− exosomes. These data revealed that Hsp70 reactivity in NK cells is inducible by Hsp70/Bag-4 surface-positive exosomes, independent of the tumor cell origin. Mean values of four independent experiments ±SE, at one distinct E/T

ratio of 10:1, were summarized in Table 2B. *C*, Hsp70/Bag-4–positive exosomes derived from Colo+ and CX+ carcinoma sublines stimulate secretion of granzyme B by CD94^{+} NK cells. CD94^{+} NK cells (2×10^6 cells/mL) were incubated with different concentrations (0.1, 1, and 10 μg protein/mL) of Hsp70/Bag-4 surface-negative and surface-positive exosomes, generated from Colo− and Colo+ carcinoma sublines. As a control, NK cells were incubated with low-dose IL-2 (100 IU/mL) alone. After 4 days, the cell-free culture supernatants were harvested and the amount of released granzyme B was quantified by ELISA. *Columns*, mean values of three independent experiments; bars, SE. *Significantly different values from control levels ($P < 0.05$).

Table 1A

Flow cytometric analysis of 7-AAD negatively gated, viable Colo−/Colo+ and CX−/CX+ carcinoma sublines

Marker	Plasma membrane–positive cells, % ± SE[*] (mean fluorescence intensity)			
	Colo−	Colo+	CX−	CX+
Hsp70	34 ± 5 (25 ± 5)	73 ± 5[†] (29 ± 7)	20 ± 6 (10 ± 4)	90 ± 8[†] (18 ± 3)
Bag-4	29 ± 11 (24 ± 2)	78 ± 1[†] (30 ± 5)[†]	42 ± 10 (8 ± 1)	78 ± 2[†] (17 ± 1)[†]
MHC I	99 ± 1	98 ± 2	98 ± 1	98 ± 2

[*] Data represent mean percentages of Hsp70 (cmHsp70.1), Bag 4 (IMG-152), and MHC I (W6/32) plasma membrane-positively stained cells of three independent experiments ± SE.

[†] Significantly different from the corresponding negative cell type ($P < 0.01$).

Table 1B

Flow cytometric analysis of latex bead–coated exosomes derived from supernatants of Colo−/Colo+ and CX−/ CX+ carcinoma sublines

Marker	Surface-positive exosomes (% ± SE)[*]			
	Colo− exos	Colo+ exos	CX− exos	CX+ exos
Hsp70	3 ± 3	84 ± 5[†]	19 ± 10	73 ± 3[†]
Bag-4	5 ± 2	69 ± 9[†]	7 ± 5	58 ± 8[†]
MHC I	98 ± 3	97 ± 3	98 ± 2	98 ± 1

Abbreviation: exos, exosomes.

[*] Data represent mean percentages of Hsp70 (cmHsp70.1), Bag-4 (IMG- 152), and MHC I (W6/32) surface-positive exosomes of three independent experiments ± SE.

[†] Significantly different from the corresponding negative cell type.

Table 2A

Specific lysis of Colo−/Colo+, CX−/CX+, and K562 target cells by differentially activated NK cells before and after blocking of the target cells with Hsp70 specific antibody cmHsp70.1

Target cells	Mean values of specific lysis (% ± SE)*					
	Control	TKD	CX− exos	CX+ exos	CX− lys	CX+ lys
Colo−	8 ± 3	19 ± 2	11 ± 6	18 ± 3	nt	nt
Colo+	12 ± 4	28 ± 4[†]	13 ± 5	30 ± 4[†]	nt	nt
CX−	15 ± 5	43 ± 2.5	55 ± 4	50 ± 4	22 ± 6	20 ± 8
CX− plus cmHsp70.1	nt	43 ± 8	48 ± 9	41 ± 5	nt	nt
CX+	19 ± 4	78 ± 5[†]	62 ± 3	83 ± 3[†]	23 ± 2	22 ± 8
CX+ plus cmHsp70.1	nt	20 ± 4[†]	59 ± 4	43 ± 4[†]	nt	nt
K562	5 ± 1	63 ± 8[†]	20 ± 3.5	53 ± 7[†]	32 ± 2	32 ± 2
K562 plus cmHsp70.1	nt	19 ± 8[†]	25 ± 6	24 ± 8[†]	nt	nt

Abbreviation: lys, lysates; nt, not tested.

*
Lysis of Colo−/Colo+, CX−/CX+, and K562 target cells at a distinct E/T ratio of 10:1, by CD94+ and CD3⁻CD19⁻ NK cells stimulated either with 100 IU/mL IL–2 only (control) or with a combination consisting of low-dose IL–2 (100 IU/mL) plus TKD (2 μg/mL; TKD), plus CX− exosomes/CX+ exosomes, or plus CX− lysates/CX+ lysates, at a concentration of 10 μg/mL each. Data represent mean values of at least three independent experiments ± SE.

†
Means significantly different from the relevant counterpart ($P < 0.005$).

Table 2B

Specific lysis of CX−/CX+ target cells by NK cells stimulated with autologous or allogeneic exosomes

Target cells	Mean values of specific lysis (% ± SE)			
	CX− exos	**CX+ exos**	**Colo− exos**	**Colo+ exos**
CX−	55 ± 4	50 ± 4	55 ± 6	42 ± 8
CX+	62 ± 3[*]	83 ± 3[†]	59 ± 4[*]	79 ± 6[†]

[*] Lysis of CX−/CX+ target cells at a distinct E/T ratio of 10:1, mediated by CD94^{+} NK cells stimulated either with IL-2 plus CX− exosomes or IL-2 plus CX+ exosomes; or with IL-2 plus Colo− exosomes or IL-2 plus Colo+ exosomes, at a concentration of 10 μg/mL each. Data represent mean values of four independent experiments ± SE. Similar results were obtained if CD3/CD19-depleted NK cells were used for stimulation.

[†] Means significantly different from the relevant counterpart ($P < 0.005$).

Table 2C

Cell surface density and fold increase in cell surface markers on CD56+ NK cells stimulated either with Hsp70 peptide TKD (2 μg/mL), CX−/CX+ exosomes (10 μg/mL), and lysates (10 μg/mL) derived thereof as compared to unstimulated NK cells

NK cell marker	Mean fluorescence intensity (fold increase)				
	TKD	CX− exos	CX+ exos	CX− lys	CX+ lys
CD94	336 (2.0)*	227 (1.3)	315 (1.9)*	241 (1.4)	241 (1.4)
NKp30	108 (2.6)*	104 (2.4)*	117 (2.7)*	101 (2.4)*	103 (2.4)*
NKp44	266 (2.2)*	293 (2.4)*	313 (2.6)*	256 (2.1)	293 (2.4)*
NKp46	342 (1.3)	320 (1.2)	354 (1.4)	347 (1.3)	333 (1.3)
NKG2D	213 (1.1)	276 (1.4)	283 (1.4)	273 (1.4)	259 (1.3)
CD69	185 (3.1)*	139 (1.8)	113 (2.4)*	119 (1.8)	118 (1.8)
CD158a	524 (1.2)	560 (1.2)	505 (1.1)	433 (1.0)	442 (1.0)

NOTE: Data represent mean values of three independent experiments.

*
Means significantly different from unstimulated controls. Similar results were obtained if CD3/CD19-depleted NK cells were used. The percentage of CD3−/CD56+ NK cells in all experiments was always greater 85%.